

Determination of the heat flux to the workpiece during dry turning by inverse methods

M. Deppermann¹ · R. Kneer¹

Received: 15 May 2015 / Accepted: 5 September 2015 / Published online: 3 October 2015
© German Academic Society for Production Engineering (WGP) 2015

Abstract Reducing metal machining costs and harmful effects to the environment are the main benefits of dry machining compared to the application of cooling lubricants during machining processes. The abandonment of any lubricants is causing higher temperatures of workpiece, chip, and tool. Thus, the temperature gradient varies with time and space over the workpiece, causing dimensional deviations and profile defects due to thermal expansion and shrinking. The aim of this work is to determine the heat flux to the workpiece from experimental data. The temperatures of the workpiece were measured during an orthogonal turning process of carbon steel (AISI 1045). An analogous thermal model is used to solve the ill-posed inverse heat conduction problem by the sequential estimation method, introduced by Beck et al. (Inverse heat conduction, Wiley, New York, 1985) and for the evaluation of the results. The heat flux to the workpiece could be used in further work as a basic boundary condition in finite element simulations to find an alternative tool path, which compensate thermally induced deviations and profile defects of the workpiece. The heat flux to the workpiece is calculated for different cutting velocities, feed rates, and the influence of TiN-coatings on cemented carbide tools. Cutting parameters have been identified to minimize the heat load on the workpiece in general and therefore reduce errors due to dry machining.

Keywords Orthogonal cutting · Heat partitioning · Thermal impact · Inverse heat conduction problem

✉ M. Deppermann
deppermann@wsa.rwth-aachen.de

¹ Institute of Heat and Mass Transfer, RWTH Aachen University, Augustinerbach 6, 52056 Aachen, Germany

1 Introduction

Dry machining of metals holds strong advantages, due to its ecological and economic benefits [1, 2]. The main disadvantage is the significant heat load on the workpiece, causing dimensional deviations and profile defects due to thermal expansion [3, 4]. To overcome these disadvantages compensation strategies are needed. One approach could be to change the tool path of CNC machines. Numerical finite element simulations of the workpiece temperature distribution and the according material expansion could evaluate the impact of different tool path corrections. In this manner the tool path could be varied until the desired workpiece dimensions are met, after the workpiece is cooled down to its initial temperature. Experimental validated boundary conditions of the heat flow rate to the workpiece as a function of cutting parameters would be needed, in addition to thermal and mechanical material properties, heat losses to the environment, heat losses to machine parts, and cutting forces [5, 6].

A different approach would be to minimize the heat load on the workpiece and keep the tool path untouched. Therefore, general knowledge of the heat dissipation and distribution of thermal energy as a function of cutting parameters are needed. The minimization of the heat load on the workpiece would reduce other temperature-stimulated effects at the same time. Uncontrolled heat treatment, and the resultant change of the micro structure, could also be reduced [7].

The heat flux to the workpiece and its dependence on cutting parameters are investigated to identify parameters causing a heat load on the workpiece. Additionally, the influence of TiN-coatings on cemented carbide tools is evaluated.

The orthogonal turning process is well suited for thermal investigations. Only the main cutting edge of the tool is in

contact with the workpiece and the complexity of the process can be simplified from a general transient 3-D problem to a transient 1-D model. The temperature distribution of the workpiece can be measured with high-speed infrared-cameras during metal turning.

The dry turning process was thermally analyzed with spatial and time resolved measurement methods in recent studies [5, 8], the orthogonal cut by a planer was measured by Heisel et al. [9]. The experimental investigations of the workpiece's thermal load from temperature measurements for different cutting parameters and tools generate a large amount of measurement data. Heat flow rates need to be determined from transient and locally distributed workpiece temperatures for each set of parameters investigated. The estimation of boundary heat fluxes based on experimental data can be treated as an ill-conditioned inverse heat conduction problem [10, 11]. Using inverse solution methods (in example the suggested sequential function specification algorithm) for the calculation of the boundary heat flux have the advantage of a low demand in computational resources.

Aurich et al. [5] reconstructed the thermal load of the workpiece by finite element simulation and comparison to the measured temperatures. The reconstruction of heat fluxes at inaccessible outer boundaries require solving an ill-posed problem, the temperature evolution do not necessarily depend steadily on the heat fluxes due to “lagging” and “damping” effects in transient heat conduction [10]. Further benefits of the present approach are a strict numerical reconstruction of the heat flux evolution without any subjective comparison of temperatures and the known accuracy of the solution.

Different machining processes, workpiece materials, and geometries have been thermally investigated recently. One example is dry down milling of AISI 4140 (42CrMo4) [12], where an experiment was compared to a finite element simulation. In a later work, the same experiment was re-evaluated by using an numerical optimization procedure to determine the heat flux into the workpiece [13]. The later approach is similar to the one pursued in the present work. However, the physics of heat generation and distribution in machining processes is not well enough understood to allow for a direct transfer of results from one process to another.

2 Objectives and procedure

The present paper focuses on the different steps to reconstruct the heat flux histories. The reconstruction of heat fluxes at inaccessible outer boundaries based on temperature measurements require solving an ill-posed inverse heat conduction problem. Therefore, a stable, accurate, and fast algorithm with little computational effort is desirable,

although not all criteria can be fulfilled completely at the same time. A complexity reduction of the real machining process and conversion into an analogous heat transfer model of lower dimensionality offers a compromise. For this purpose, the heat transfer characteristics, the symmetry plane, isotherms, and area of induced heat needs to be identified. The main steps of the proposed approach can be structured as follows:

1. Identification of dominant heat transfer mechanism
2. Building an analogous heat transfer model
3. Implementing a stable, accurate, and fast solution algorithm.

In the next subsections the experimental procedure and set-up is summarized for an understanding of the orthogonal turning process and the measured data. Afterwards, the conversion of the dominant heat transfer mechanism into the analogous heat transfer model is described. In the last subsection the implemented solution algorithm is tested for its computing time, accuracy and stability.

2.1 Experimental set-up

The numerical investigation of this work is based on experimental data, that has been published in the proceedings of the 15th international heat transfer conference [8]. In this work, the orthogonal turning process without any cooling lubricants has been investigated. Orthogonal cutting can be considered two dimensional and is geometrically simple (see Fig. 1). Within one rotation of the workpiece, the diameter is reduced twice the feed f , which happens to be equal to the uncut chip thickness h for the present process. The uncut chip width and the workpiece width b are equal as well. The cutting speed v_c is equivalent to the tangential velocity of the workpiece at the outer diameter D . Thus, the heat generation due to deformation and friction is mainly influenced by uncut chip width, cutting speed, feed rate and materials for the tool and workpiece.

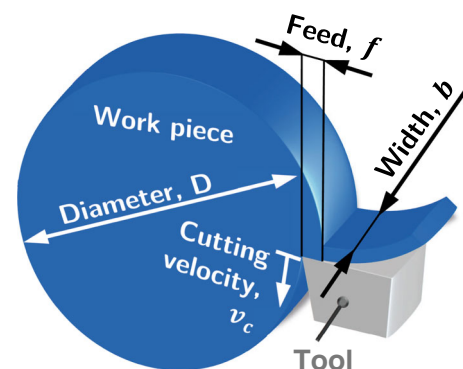


Fig. 1 Set-up of the orthogonal turning process

Therefore, the influence of cutting velocities and feed rates on the workpiece temperatures have been investigated for uncoated cemented carbide inserts (Sandvik N151.2-540-40-3B H13A) and coated inserts (TiN-coating layer of 4 μm). The tools had a rake angle of 0° , a relief angle of 10° and the substrate consists of 94 m% WC and 6 m% Co. The cutting edge radius r_β was 25 μm . Metal disks out of carbon steel AISI 1045 in normalised state (C45E+N, Mat.No. 1.1191) were cut with constant cutting velocity and feed rate (compare Fig. 1). The initial diameter of each circular workpiece was 180 mm, with a width of 3 mm.

The experimental set-up was installed on a lathe with a fixed tool and a free moving workpiece, the lathe *Weisser Frontor M1*. Thus, this set-up enabled a free and fixed measurement area on the front face of the workpiece (see Fig. 2).

A high-speed infrared (IR) camera was fixed perpendicular to the workpiece's front surface, providing a temporal resolution of 1250 Hz and a temperature resolution of 25 mK at 25 $^\circ\text{C}$. The optical resolution was 195.5 $\mu\text{m}/\text{pixel}$. The camera uses a MCT-detector (mercury cadmium telluride) sensitive to infrared radiation in the wavelength range of 3.7 to 4.8 μm . The MCT-detector is cooled down to 76 K to increase its sensitivity and to minimize its self-radiation.

The measurement accuracy of the camera is below 0.1 K to record temperature change, since the noise equivalent temperature difference (NETD) is 25 mK. To account for the influence of heat radiation of the tool and chip, the temperature measurement accuracy of the experimental set up is estimated to be 1 K to detect the temperature change of the workpiece.

The workpiece has been coated with paint without any metallic substances and temperature resistant up to roughly 600 $^\circ\text{C}$. In this manner the surface of the workpiece was considered as a grey emitter with high emissivity of 0.972. The emissivity of the paint has been determined for the presented infrared camera by comparison of the steady-state heat radiation between heated paint and a black body of the same temperature.

Within the camera's field of view, a measurement area has been evaluated 0.394 mm apart from the cutting edge

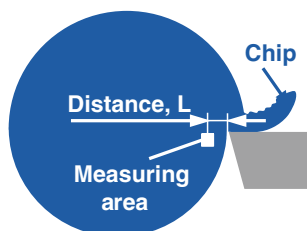


Fig. 2 Position of temperature measurement on the workpiece front face with distance $L = 0.394$ mm

of the tool (see Fig. 2). The distance L was read off the thermographic video, with an accuracy of ± 97.7 μm . The measurement position was chosen closest to the cutting edge with marginal disruptions during the machining.

2.2 Experimentation

A new workpiece with an initial diameter of 180 mm and a separate cutting tool was mounted for each measurement. The temperature evolution was recorded over the first 5 s for each parameter variation of cutting velocity (100, 125 and 150 m/min), feed (0.05, 0.10 and 0.20 mm), and the two different tools (un-/coated). Each parameter variation was repeated twice with constant parameters. An inverse heat conduction problem has been solved for the resulting 54 data sets to determine the induced transient heat flux at the cutting edge. The thermal model and numerical procedure necessary for the heat flux determination is explained in the next two sections.

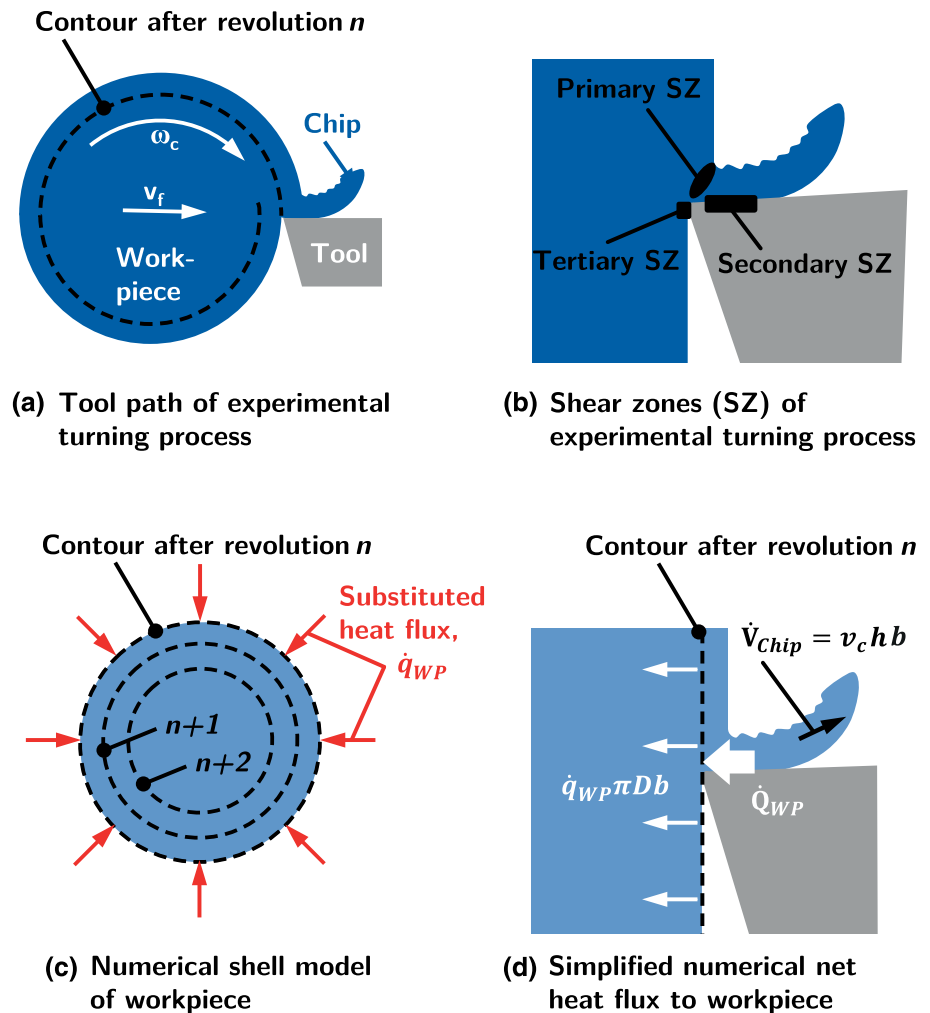
2.3 Analogous thermal model

The real orthogonal cutting process (see Fig. 3a, b) has been transferred into an analogous thermal model for the numerical investigation (Fig. 3c, d). The tool path of the real process can be described by an Archimedean spiral (a). Dissipated heat flows from the three different shear zones, the primary, the secondary, and the tertiary (see Fig. 3b) to the chip, the tool, and the workpiece, if heat losses to the environment are neglected. The heat load on the workpiece results of the combined dissipated heat flow rates of the primary, the secondary, and marginally of the tertiary shear zone. By measuring the workpiece temperatures at the area illustrated in Fig. 2 the total heat load on the workpiece can be calculated. In order to differentiate the heat flow rate by the shear zones the temperature distribution next to each shear zones needs to be measured.

The analogous thermal model, used to calculate the heat flux to the workpiece, is related to the ideal circular outer surface of the disk for each revolution, illustrated in Fig. 3c. The outer diameter of the disk is reduced stepwise twice the feed for each revolution. In this manner the continuous tool path is transferred into a stepwise cutting process. The heat flux to the workpiece is assumed to be uniform over the idealized outer diameter in radial direction. This is the net heat flow rate to the workpiece \dot{Q}_{WP} , without the enthalpy flow rate of the chip and heat loss to the environment of the shear zones (see Fig. 3d).

Finally, the continuous heat transfer of the dry orthogonal cut with three different local heat sources is transferred into a stepwise cutting model with uniform heat flow rate for each cutting step. The heat flow rate can vary over

Fig. 3 Heat transfer model of the dry orthogonal turning process



time in terms of changing from step to step in the introduced shell model. The resulting transient 1-D heat conduction model is utilized by the solver described in the section.

2.4 Calculation of heat fluxes

The temperature distribution over time is known due to the measurements at distance L (see Fig. 2), and the boundary conditions at the outer diameter are unknown. In other terms the temperature evolution is known inside the domain of the workpiece and the heat flux at the boundary is sought. Therefore, an inverse problem is formed and it is necessary to calculate from an “effect” back to the “cause” [14]. The accuracy of the backwards calculated heat flux is verified in the next subsection. Any boundary inverse heat conduction problem is very sensitive to temperature measurement errors and unavoidable noise, resulting in an ill-posed problem [10, 11].

The ill-posed inverse heat conduction problem is solved by a sequential function specification algorithm with future

times regularization as described by Beck et al. [10]. The proposed solver works without any iteration and determines heat flux histories according to 6250 time steps in 0.73 s in Matlab R2015a running on a Windows desktop computer with 3.4 GHz.

The proposed solver is based on the Stolz algorithm that utilizes a numerical approach to solve the heat conduction equation. Therefore, the heat conduction equations is reformed by the Duhamel’s theorem. The Stolz algorithm determines the exact solution to a surface heat flux due to a temperature change inside a body. If the heat flux histories are known, future heat fluxes can be estimated in a sequential manner. The algorithm is marching through the time domain of given temperatures and is calculating the accordant heat flux step by step. Beck included an estimation method of future times for each time step to minimize the least-squares of calculated and measured temperature. The future time steps approach serves as a “damping” mechanism, which stabilizes the solution. Thus, the resulting sequential function estimation algorithm can handle noisy measurement data.

The implemented solver is limited to 1-D transient heat conduction cases with constant material properties. The initial condition is a uniform temperature field and an adiabatic boundary on the opposite side of the heat flux to be estimated. The unknown heat flux needs to be a function of time only and convective heat losses were neglected. For more complex heat conduction cases, 2-D geometries for example, a reduction of the conduction dimensions would be needed.

2.4.1 Verification of the solver

The solver has been compared to a two dimensional numerical solution for a solid cylinder with constant heat flux at the outer radius taken from literature [15]. Such a comparison to a numerical solution of a test case avoids any so called *inverse crime*, as the reconstruction of the heat flux on the same computational grid or using parts of the solver itself calculating the temperature evolution [16]. The test case set-up is designed in a similar manner as the set-up and data acquisition of the experiments. Geometrical dimensions, the distance of the measuring area to the outer rim of the cylinder, and the data sampling rate are equal to the experimental case.

The exact temperature distribution is calculated at distance L for a step increase in the surface heat flux of 100 kW/m^2 . The exact temperature distribution serves as pseudo measurement data and therefore is used to reconstruct the according heat flux histories by the solver. Figure 4 shows the solution of the implemented sequential function specification solver and the exact numerical solution of the test case. The relative mean error over all data points between the exact solution and the solver is -0.0051% for the temperature and 1.64% for the heat flux. The temperature is underestimated and the heat flux overestimated. Further, the adverse sensitivity of inverse boundary conduction problem is represented by the 200

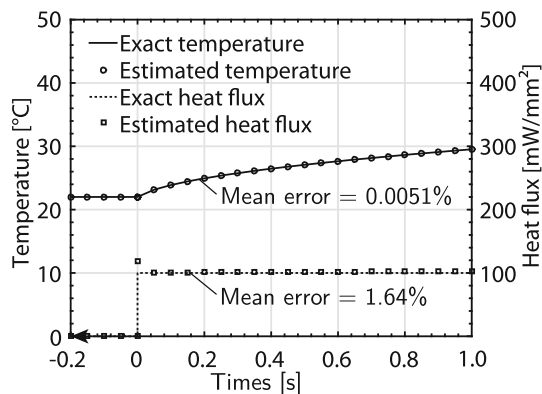


Fig. 4 Verification of the solver by comparison to an exact numeric solution

times higher heat flux error, which is still small. This difference in the relative error illustrates the importance of a methodical procedure to solve the inverse heat conduction problem.

The root mean squared error, generally referred to as RMSE, is equal to 0.0051% for the temperature. Thus, the temperature solution has very little noise and is a little bit underestimated at all times. The RMSE of the heat flux is 2.81% . Thus, the solver is stable even for an instantaneous step-wise heat flux increase.

3 Results and discussion

The heat flux to the workpiece is evaluated by the inverse method over the duration of each parameter variation and finally averaged over time. The results are plotted in Fig. 5 for the different tools, cutting velocities, and uncut chip thickness or feed respectively. The heat flux rises proportionally over the feed and cutting velocity. The evolution of the heat flux over the feed shows an overall asymptotic trend for each cutting velocity. The TiN-coated cemented carbide tools decrease the heat load on the workpiece by -37.2% averaged over all data points.

Tables 1 and 2 show the values of Fig. 5 and can be used as a reference for boundary conditions in finite element simulations. The variation of the tool path during dry machining could be simulated to compensate dimensional deviations for a specific workpiece and machining operation.

By normalizing the net heat flow rate to the workpiece, \dot{Q}_{wp} , using the volumetric flow rate of the chip, \dot{V}_{chip} a volumetric heat source can be determined, called the heat load on the workpiece, ϕ_{wp} . The heat load gives the amount of heat transferred to the workpiece by removing material for a specified time and can be defined as,

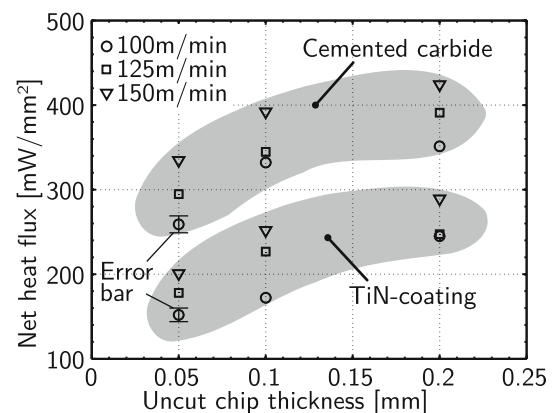


Fig. 5 Net heat flux to the workpiece for different cutting velocities as a function of uncut chip thickness or feed respectively; grey areas mark same tool type

Table 1 Net heat flux for cemented carbide tools for different uncut chip thicknesses, h and cutting velocities, v_c

		Net heat flux, \dot{q}_{wp} [mW/mm ²]			
		h	0.05 mm	0.10 mm	0.20 mm
v_c	100 m/min		259.1	332.0	351.3
	125 m/min		294.8	344.7	391.0
	150 m/min		334.6	392.1	424.2

Table 2 Net heat flux for TiN-coated cemented carbide tools for different uncut chip thicknesses, h and cutting velocities, v_c

		Net heat flux, \dot{q}_{wp} [mW/mm ²]			
		h	0.05 mm	0.10 mm	0.20 mm
v_c	100 m/min		152.0	172.3	245.0
	125 m/min		178.0	226.8	247.3
	150 m/min		200.9	251.9	289.2

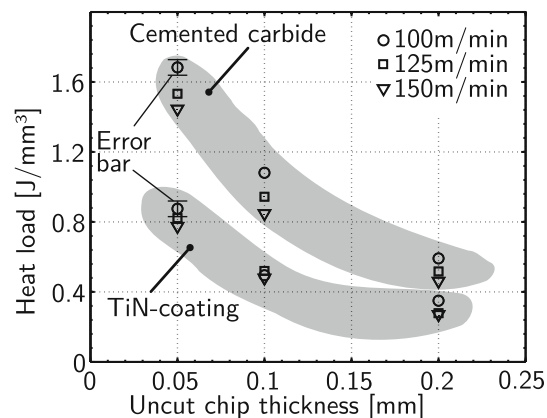
$$\phi_{wp} = \frac{\dot{Q}_{wp}}{\dot{V}_{chip}} = \frac{\dot{q}_{wp}\pi D}{v_c h} \quad (1)$$

The heat load per unit volume removed can be used to calculate the total heat load on the workpiece for a complete process step, for example machining from an initial to a final diameter in orthogonal turning. Thus, the minimal heat load on the workpiece for different cutting parameters can be identified in general by direct comparison.

The heat flow or heat flux is not an ideal measure, as it does not account for the cutting velocity, feed rate or other parameters to determine the speed of the production process. Thus, despite lower heat flows, slow cutting velocities may generate more heat as the workpiece is exposed to the heat flow for a longer period of time.

A more useful measure is the heat load per volume removal rate, or the heat load per volume removed. In an adiabatic case, the heat load can be translated in a temperature load in the workpiece. As a change in cutting velocities leads to a variation of both, the heat load and the volume removal rate, any change in duration of the production process is accounted for.

Figure 6 indicates that the heat load decreases over uncut chip thickness and over cutting velocity. The heat load is inversely proportional to the cutting parameters, which seems to be in contradiction to the ascending heat fluxes over the chip thickness in Fig. 5. But by raising the cutting velocity for a fixed chip volume, the total machining time goes down and therefore the heat flow rate rises. The applied TiN-coated tool reduces the amount of

**Fig. 6** Volumetric heat source, ϕ_{wp} , of the workpiece per chip volume for different cutting velocities as a function of uncut chip thickness or feed respectively; grey areas mark same tool type

heat significantly (in average by -43.2%). Thus, a general approach to minimize the total heat load for a complete machining operation is to raise the cutting parameters and to use coated cemented carbide tools.

Exemplary error bars have been added to the plot and include the uncertainty of the location ($\pm 97.7\ \mu\text{m}$) as well as the uncertainty of the temperature measurement of $\pm 1\ \text{K}$.

The volumetric heat source seems to depend more on uncut chip thickness, than on cutting velocity. In addition, the characteristics of each cutting velocity are asymptotic and tend to approach a minimum. For further understanding of the influence of the feed rate and cutting velocity and their combination on the orthogonal turning process, the Péclet number is used to compare the enthalpy transport along the chip to the heat conduction towards the workpiece. The Péclet number is defined as

$$Pe = \frac{h v_c}{\alpha} \quad (2)$$

where h is the uncut chip thickness, which is equal to the feed f in the present case. v_c is the cutting velocity and α is the thermal diffusivity of the workpiece material.

In Fig. 7 the volumetric heat source is plotted over the Péclet number. The characteristic for the tools tends to minimum at Péclet numbers clearly >30 . The heat dissipating in the primary and secondary shear zones is transported mainly by the convective enthalpy flow along the chip. Thus, the heat load on the workpiece decreases with higher cutting velocities and feed rates.

The graph for the uncoated tool reaches a minimum of approximately 400 and of 200 MJ/m³ for the TiN-coated tool. The position of the tertiary shear zone is between the tool edge and the workpiece, and thus the dissipating heat due to friction can barely be transported along the formed chip. The comparison of both tools indicate that the friction

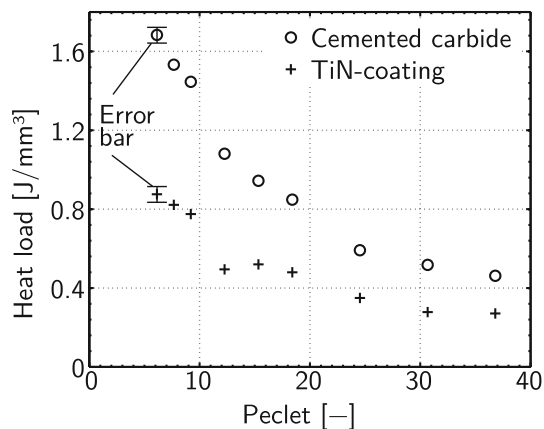


Fig. 7 Volumetric heat source of the workpiece per chip volume for different Péclet numbers

of the secondary and tertiary shear zones seemed to be reduced by the TiN-coating.

4 Conclusion

Based on experimental data the heat load on the workpiece during orthogonal turning has been calculated. The resulting heat flux to the workpiece has been determined in dependence of feed rate and cutting velocity. Additionally, the influence of a TiN-coating on a cemented carbide tool has been investigated. The results can be utilized for finite element simulations of dry turning processes that aim at the thermal-elastic behavior during different machining steps. Further, the variation of tool paths could be simulated for a specific turning task to compensate the profile defects and dimensional deviations due to the warming of the workpiece.

A more general approach is to minimize the heat load on the workpiece by using cutting parameters of high Péclet numbers. The results for cemented carbide tools show that raising the Péclet number from 6.1 to 36.8 reduces the volumetric heat source of the workpiece by -72.6% . Using the same tool with a TiN-coating for the same Péclet number of 36.8 reduces the heat source for an orthogonal turning process by -30.0% .

Acknowledgments The authors would like to thank the German Research Foundation (Deutsche Forschungsgemeinschaft, DFG) for

the funding of the depicted research within the priority programme 1480 (SPP 1480). Further, the authors would like to thank Prof. Klocke and Hendrik Puls of the Laboratory for Machine Tools and Production Engineering (WZL), RWTH Aachen, for providing the turning machine and the support in performing the experiments.

References

- Klocke F, Eisenblätter G (1997) Dry cutting. *CIRP Ann Manuf Technol* 46(2):519–526
- Weinert K, Inasaki I, Sutherland JW, Wakabayashi T (2004) Dry machining and minimum quantity lubrication. *CIRP Ann Manuf Technol* 53(2):511–537
- Bryan J (1990) International status of thermal error research (1990). *CIRP Ann Manuf Technol* 39(2):645–656
- Weck M, McKeown P, Bonse R, Herbst U (1995) Reduction and compensation of thermal errors in machine tools. *CIRP Ann Manuf Technol* 44(2):589–598
- Aurich JC, Zimmermann M, Schindler S, Steinmann P (2014) Analysis of the machining accuracy when dry turning via experiments and finite element simulations. *Prod Eng* 8(1–2):41–50
- Klocke F, Lung D, Puls H (2013) FEM-modelling of the thermal workpiece deformation in dry turning. *Proced CIRP* 8:240–245
- Brinksmeier E, Brockhoff T (1996) Utilization of grinding heat as a new heat treatment process. *CIRP Ann Manuf Technol* 45(1):283–286
- Deppermann M, Puls H, Burghold ME, Kneer R, Klocke F (2014) Experimental investigation of the work piece temperatures in dry orthogonal metal turning. In: Proceedings of the 15th international heat transfer conference, Begell House, Kyoto, Japan, no. 9223 in IHTC15
- Heisel U, Storchak M, Krivoruchko Dmitrii (2013) Thermal effects in orthogonal cutting. *Prod Eng* 7(2–3):203–211
- Beck JV, Blackwell B, Clair CRS (1985) Inverse heat conduction. Wiley, New York
- Alifanov OM (1994) Inverse heat transfer problems, 1994. Springer, New York
- Sölter J, Gulpak M (2012) Heat partitioning in dry milling of steel. *CIRP Ann Manuf Technol* 61:87–90
- Wernsing H, Gulpak M, Büskens C, Sölter J, Brinksmeier E (2014) Enhanced method for the evaluation of the thermal impact of dry machining processes. *Prod Eng* 8(3):291–300
- Maillet D (2014) Experimental inverse problems: potentials and limitations. In: Proceedings of the 15th international heat transfer conference, Begell House, Kyoto, Japan, no. KN10 in IHTC15
- Carslaw HS, Jaeger JC (1959) Conduction of heat in solids, Second edn. Oxford University Press, Oxford
- Mueller JL, Siltanen S (2012) Linear and nonlinear inverse problems with practical applications. Society for Industrial and Applied Mathematics, Philadelphia